2009-32-0021 / 20097021

Effect of spark assistance on improving cyclic stability of auto-ignition at light load in a small two-stroke engine

Janitha Wijesinghe, Guang Hong
University of Technology, Sydney

ABSTRACT

Cyclic instability is a common problem in the operation of conventional two-stroke spark-ignition engines. Previous research has shown that auto-ignition (AI) could help solve this problem. However, at light engine loads, even under AI, the cyclic instability may still be significant due to the difficulty in maintaining the minimum temperature required by AI. Despite the benefits brought by AI in fuel consumption and emission reduction, the high level of cycle-to-cycle variation at light load may delay the realization of AI operation in engine products. To solve this problem, spark assistance has been identified as a cost effective and convenient way to improve the stability of AI operation at light load. This paper aims to report our experimental investigation to the effectiveness of spark assistance on cyclic variation of AI at light engine load conditions.

INTRODUCTION

Previous researches into the use of auto-ignition (AI) in two-stroke small engines have shown the ability of improving cyclic irregularities, drastic reduction of HC emissions and achieving better fuel consumptions [1,2]. However controlling of AI timing and the lack of thermal energy at lower loads are two major challenges that have to be overcome, in order to make such AI engines viable for a wide range of applications. Spark assisted AI has been one of the approaches investigated with the aim of tackling these issues [3-7]. An electric spark has the potential to meet these challenges by providing thermal energy into the cylinder at a distinct point of time.

Wang et al investigated the effect of SI on HCCI combustion on a gasoline direct injection four-stroke engine [3, 4]. Their results showed that at the lower limit of the HCCI operating envelop, which they termed as HCCI critical status, SI was able to improve the combustion stability. It also showed that the SI triggered global HCCI in the region misfiring occurred without the spark. It was concluded that the stable HCCI combustion was realized when the mixture temperature and concentration near the top dead center (TDC) exceeded HCCI-CS. Glewen et al investigated the combustion characteristics on spark-assisted HCCI using a 'Double Weibe Function' approach proposed by them [6]. They used this method to study the role of SI and HCCI that may occur within the same cycle.

The effect of spark assisted AI on two-stroke gasoline engine was investigated by the authors focussing mainly on the high load region of AI [7]. The aim of this work is to study the effect of spark assistance on AI at its lower load boundary. At lower load region the internal EGR does not have sufficient thermal energy to reach the entire mixture temperature to AI level. Thus as the operating load reduces under AI mode, misfire would occur leading to cyclic fluctuations. At these loads when the spark plug was enabled, the cyclic fluctuations were significantly reduced. The role of the spark in this respect was investigated through the analysis of in-cylinder pressure.

EXPERIMENTAL SETUP

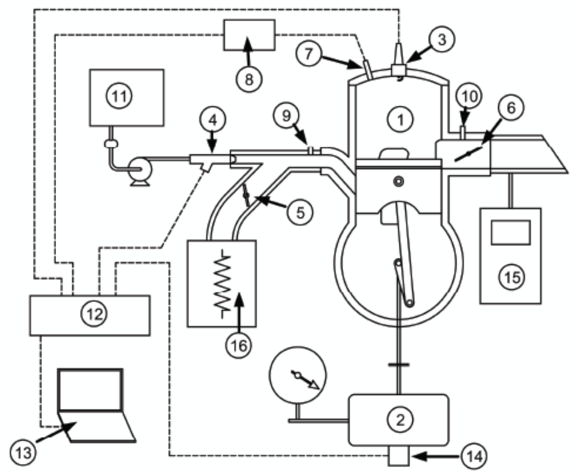

1-Test engine 2-Dynamometer 3-Spark plug 4-Fuel injector 5-Intake valve 6-Exhaust valve 7-Pressure transducer 8-Charge amplifier 9-Intake thermocouple 10-Exhaust thermocouple 11-Fuel supply system 12-Microcontroller 13-Data acquisition computer 14-Incremental rotary encoder 15-Exhaust gas analyzer 16-Intake heater chamber

Figure 1: Experimental Apparatus

Figure 1 illustrates the experimental apparatus used in this work. A 160cc piston ported single-cylinder two-stroke engine was used for this investigation. Its key specifications are listed in Table 1. A Heenan-Froude hydraulic dynamometer was used to measure the brake torque output of the engine. The cylinder pressure was measured by A PCB 112B pressure transducer and a Kistler 504-E charge amplifier. The pressure data was acquired at every degree of crank rotation with a NI data acquisition system. Intake and exhaust temperature values were recorded using K type thermocouples. An Autodiagnostics exhaust gas analyzer was used to measure the HC, CO, CO_2, NO, O_2 and the air to fuel ratio (AFR). More details about the experimental set are provided in [7].

Table 1: Engine Specification

Engine type	Two-stroke; Schnurle
Bore	61.5 mm
Stroke	56 mm
No. of transfer ports	2
Trapped compression ratio	6.7:1
Exhaust port opening angle	105.9^o ATDC
Transfer ports opening angle	117.8^o ATDC
Fuel induction system	Intake pipe injection

Fuel injection and the firing of the spark plug were controlled using a PIC microcontroller. An incremental rotary encoder with 360 pulses per revolution was used to determine the instantaneous angular position of the crankshaft. The output of the encoder was used as an external clock to drive the microcontroller which determined the spark ignition timing and fuel injection pulse width.

Gasoline (RON – 91) premixed with lubricant oil was injected into the intake manifold using a low pressure fuel injector. Fuel injection pressure was maintained at 300kPa. A butterfly valve was mounted in the intake pipe, upstream of the fuel injector, in order to vary the air flow rate. The intake valve opening rate was defined as a fraction of the projected valve opening area and the cross sectional area. AI was achieved internal EGR using a butterfly valve mounted 60mm downstream of the exhaust port [7]. The rate of exhaust restriction on the exhaust flow was defined as the fraction of the valve disk area projected in the axial direction of the exhaust pipe to the cross sectional area of the exhaust pipe.

RESULTS AND DISCUSSION

OPERATING REGION OF AI – Figure 2 illustrates the AI operating region of the experimental engine. Unlike normal SI conditions, under AI mode due to the high level of retained internal EGR, the amount of fresh charge that can be aspirated into the combustion chamber becomes limited. This in turn limits the maximum achievable BMEP leading to the AI upper limit shown in Figure 2.

For the tested engine the AI lower limit was indicated by the BMEP as shown in Figure 2. As the intake throttle opening was reduced the BMEP and the exhaust gas temperature reduced to a level lower than that required by AI. Thus the cyclic irregularities increased and resulted in misfire when the engine reached the lower limit of AI operation.

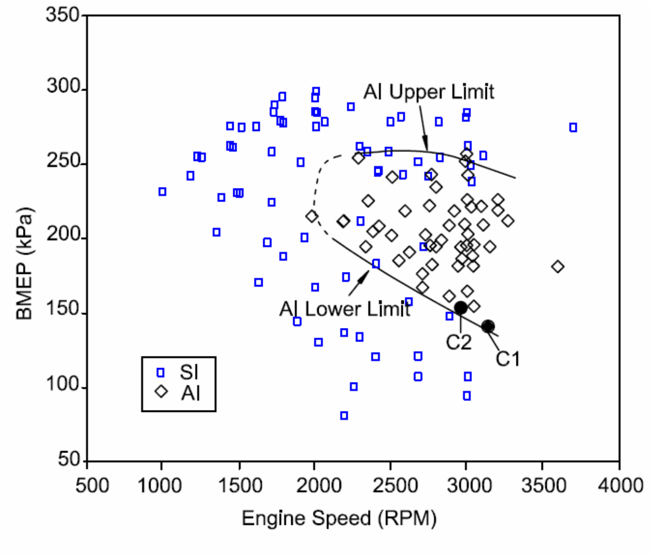

Figure 2: AI operating region

Two engine test conditions in AI mode were selected as follows:

C1. BMEP of 140 kPa and 3150 RPM and

C2. BMEP of 150 kPa and 2970 RPM

The C1 and C2 conditions are indicated by solid circles in Figure 2. C1 was selected as a condition on the AI lower limit as shown in Figure 2, aiming to investigate the effect of spark assistance on the cyclic variation at light engine loads. In this condition, the engine was able to run marginally at the AI lower limit without spark assistance. C2 was selected as a condition slightly above the AI lower limit, aiming to investigate the effect of spark timing on spark assisted AI. In the first test condition, the original magneto spark ignition was used with a fixed spark timing of 22^0 before TDC. To reach the aim of the second engine test condition, an electronic control system was developed to vary the spark timing. Results of AI with and without spark assistance will be compared in the following discussions.

In order to represent the ignition timing or the onset of AI, the relative crank position corresponding to the occurrence of 10% MBF was used. The 10% – 90% MBF duration was used as an indication of the combustion duration.

SPARK ASSISTANCE IN LIGHT-LOAD AI – Results shown in Figures 3 - 5 were based on data acquired from 28 consecutive engine cycles in test condition C1. The air to fuel ratio (AFR) was maintained at 16:1 and the spark was activated at 22^0 BTDC. In Figure 3, the cylinder pressure traces were compared in AI mode with (a) and without (b) spark assistance. The coefficient of variation (CoV) of peak pressure was used to quantitatively evaluate the change in cycle-to-cycle variation of SA-AI mode was 8.5%, whereas for the AI mode, the CoV was 14.5%.

The CoV is defined as:

CoV = (Standard deviation/Average) X 100%

The results in Figure 3 show clearly that the cycle to cycle variation of the peak pressure is reduced when the engine runs in AI mode with spark assistance than that in AI only mode, as the CoV of the peak pressure is 14.5% in the AI mode but reduced to 8.5% in SA-AI mode.

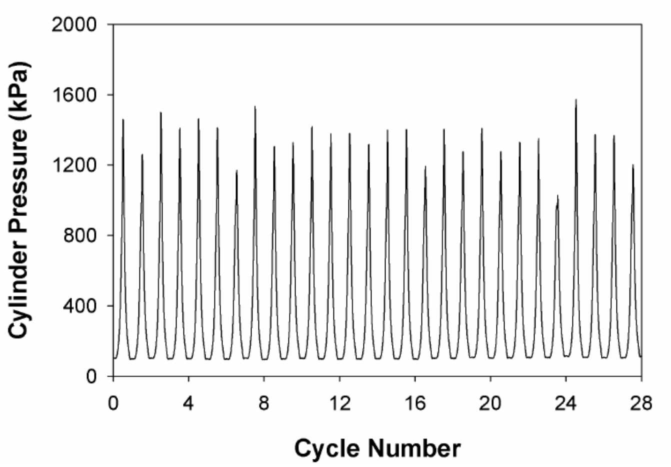

(a)

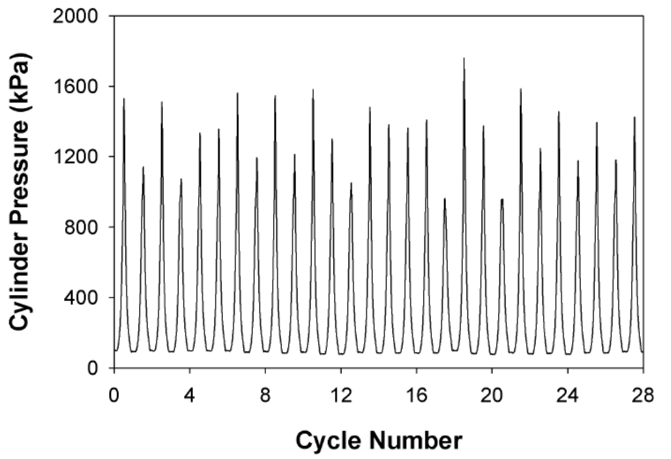

(b)

Figure 3: Cylinder pressure in test condition C1, (a) SA-AI, spark timing 22^0 BTDC and (b) AI without spark assistance

Figure 4 illustrates two histograms of 10% MBF timing under SA-AI and AI modes. The frequency of occurrence of the 10% MBF timing of the AI mode is distributed within a crank angle range of 6^0 before and 8^0 after TDC. On the other hand in the SA-AI mode the 10% MBF occurrences over the 28 cycles are mostly concentrated within a crank angle range of 1^0 before and 2^0 after TDC. Thus the SA-AI mode shows a substantial improvement in the ignition timing with respect to that of the AI mode. The standard deviations of the 10% MBF timing for SA-AI mode and AI mode tests in condition C1 were 3.1^0 and 5.4^0 respectively.

Figure 5 shows the histograms of the IMEP of the SA-AI and the AI modes. As shown in Figures 5(a) and 5(b), the cyclic behaviour of IMEP has been slightly improved by the application of SA-AI mode. The CoV of IMEP for the SA-AI and the AI mode cases were 3.5% and 6.5% respectively. The cyclic behaviour of the IMEP in AI mode seems less effected by the spark assistance, compared with the results of cylinder peak pressure and the 10% MBF timings in Figure 3 and Figure 4.

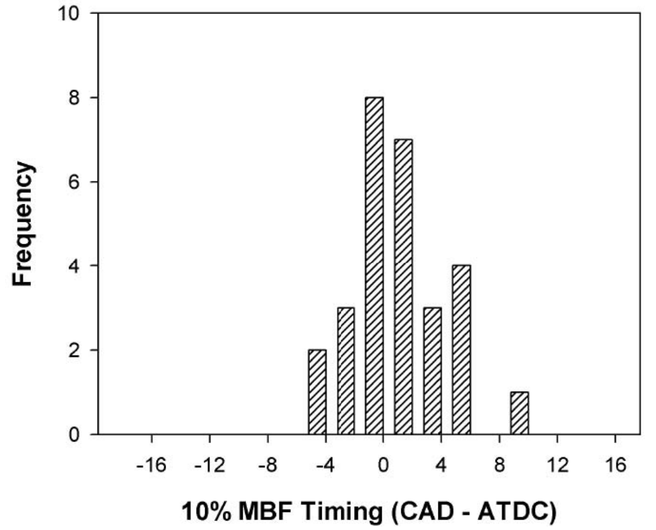

(a)

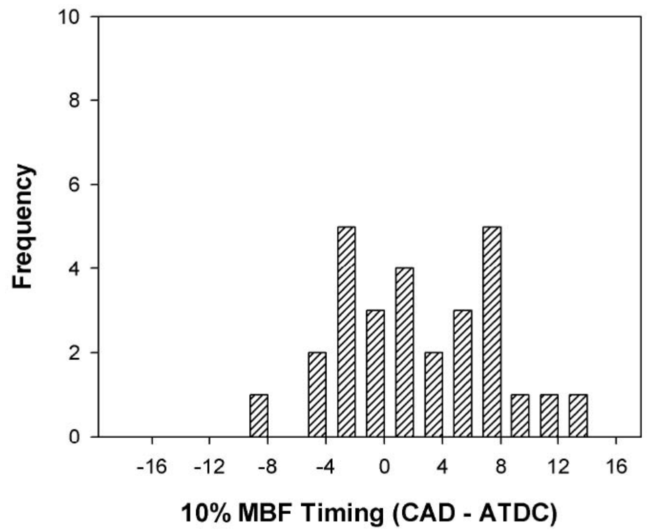

(b)

Figure 4: Histograms of 10% MBF timing in test condition C1, (a) SA-AI, spark timing 220 BTDC and (b) AI without spark assistance

Figures 3(b) and 4(b) show high cyclic variations in the peak pressure and 10% MBF timing under AI mode. This could be caused by the cyclic variation of the in-cylinder temperature and the chemical composition of the mixture at the AI lower limits. In Figure 3(b) there are several engine cycles which do not demonstrate a substantial pressure rise as the other cycles do. These cycles are associated with a delayed 10% MBF timing and a slow combustion or a relatively longer combustion duration. As shown in Figure 4(b), the 10% MBF of the late igniting cycles occurs around 10^0 to 14^0 after TDC. It is followed by a longer combustion duration (10% - 90% MBF) of over 20^0 of crank angles as shown in Figure 6, which illustrates the correlation between the 10% - 90% MBF and the 10% MBF timing. It shows that, as the 10% MBF is retarded, the combustion duration increases resulted from a slower combustion. The slow burning cycles may involve incomplete combustion leaving partially reacted intermediate compounds inside the cylinder for the next cycle. As such the following cycle usually occurs explosively with a little boost given by the heat of the trapped gas. This cycle would be characterised by complete combustion leaving no intermediate reactants for the next cycle.

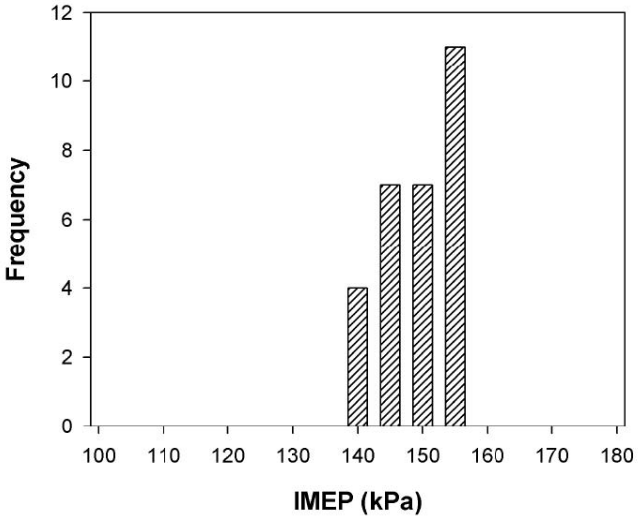

(a)

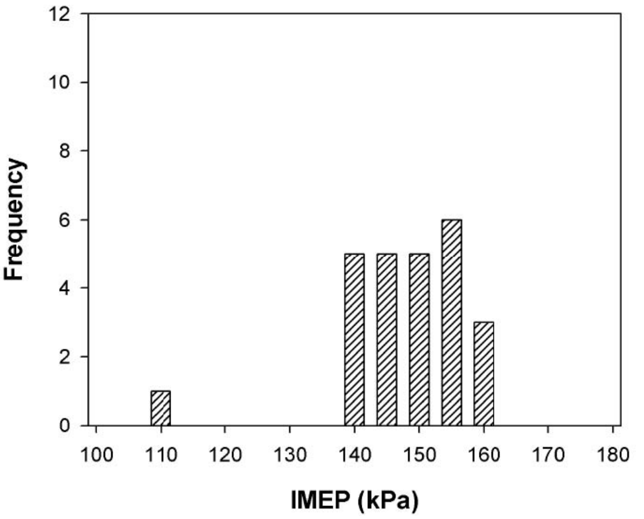

(b)

Figure 5: Histograms if IMEP in test condition C1, (a) SA-AI, spark timing 220 BTDC and (b) AI without spark assistance

The logarithmic P vs V traces for such a partially reacted cycle and a fully reacted one are shown in Figure 7. As the overall heat release is quite low, even the fully reacting cycles may not produce enough internal EGR to meet the AI temperature requirement for the following cycle. Further due to the complete combustion the subsequent fraction of internal EGR may not be enriched with intermediate reactants to supplement the shortage of thermal energy to initiate AI. As a consequence, the next cycle would unlikely result in a complete combustion, which would lead to a repetition of the sequence of fully and partially reacting cycles.

This may help explain the results of IMEP in Figure 5. In AI only mode, some of the cycles in the 28 consecutive cycles measured showed significant cyclic variation in peak pressure and 10% MBF timing. As analyzed above, they were associated with delayed 10% MBF timing followed by relatively slow combustion. However, the IMEP based on the integrated power generated in those cycles might not be so different as that in other cycles with the similar level of completion of combustion. Therefore, the effect of SA-AI mode on IMEP may not be as significant as that on the peak cylinder pressure and 10% MBF. Table 2 compares the results of the SA-AI and AI mode operations under condition C1.

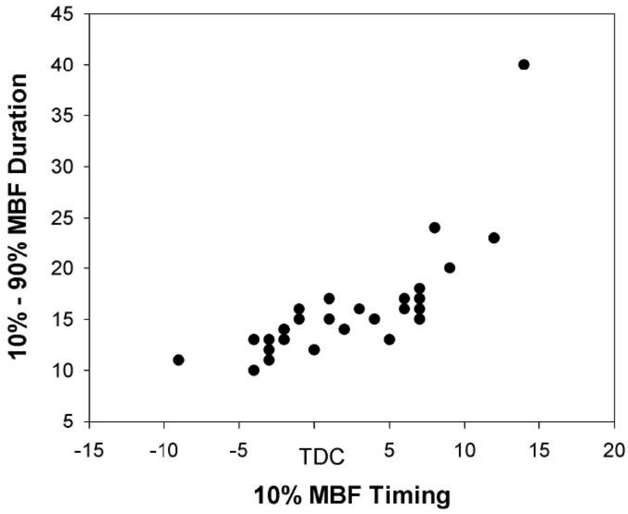

Figure 6: Correlation of 10% - 90% MBF duration with 10% MBF timing for AI mode

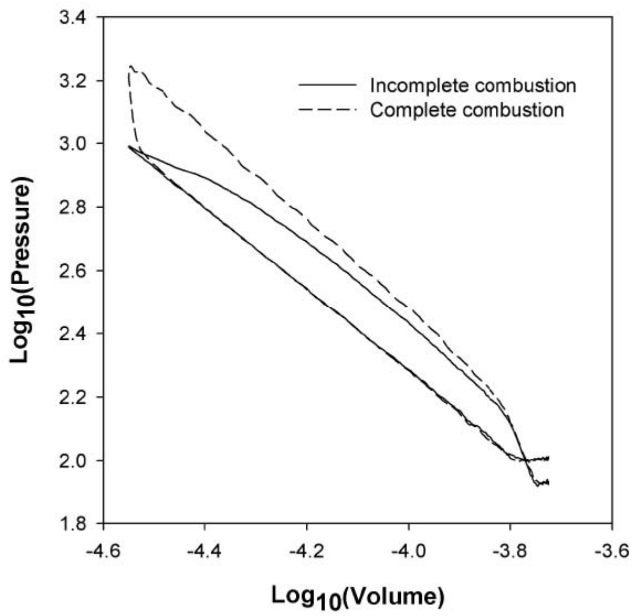

Figure 7: Log_{10}(Pressure) vs Log_{10}(Pressure) curves for partially reacted and fully reacted cycles at lower load AI mode. Test condition C1.

Table 2: Condition C1 summary

	SA – AI Mode	AI (without SA)
CoV of peak pressure	8.5%	14.5%
CoV of IMEP	3.5%	6.5%
Standard deviation of 10% MBF timing	3.1^0	5.4^0

EFFECT OF SPARK TIMING ON SA-AI – In Test condition C2 included the following three cases

- AI – AI without spark assistance
- SA-AI-22 – Spark assisted AI. SI timing at 22^0 before TDC
- SA-AI-45 – Spark assisted AI. SI timing at 450 before TDC

For all three cases the approximate speed and BMEP were 2970RPM and 150kPa respectively. The air to fuel ratio (AFR) was maintained at 15.5:1. Data were acquired from 25 consecutive cycles. The histograms of IMEP for the three cases in C2 are compared in Figure 8. As a result of comparison, the IMEP in SA-AI-45 case shows a lower cyclic variation than that in other two cases while the difference in cyclic variation in other cases is not significant. The corresponding CoV for AI, SA-AI-22 and SA-AI-45 were 10.8%, 10.4% and 6.6% respectively.

Figure 9 compares the histograms of 10% MBF timing for the three cases in test condition C2. Consistent with the comparison result in Figure 8, the spark assisted AI in SA-AI-45 case shows more effectiveness on improving the cyclic variation of 10% MBF timing than that in other two cases. The comparison in this figure also shows lesser significance of SA-AI-22 on improving the cyclic variation. The standard deviations of the 10% MBF timing for AI, SA-AI-22 and SA-AI-45 were 4.7^0, 3.4^0 and 2.7^0 respectively.

In test condition C1, the 10% MBF timing occurred within -5^0 and $+8^0$ from TDC as shown in Figure 3. At that load condition (140 kPa BMEP), the spark timing at 22^0 before TDC had a significant effect on reducing the cyclic variation of peak pressure and 10% MBF timing. This means that the spark was an initiative to promote the chemical reactions by providing the necessary heat energy. However the 10% MBF timing for all three cases in C2 lie within the range of 12^0 to 2^0 before TDC, which is relatively advanced compared to that in C1. Also the advanced 10% MBF timing in C2 indicates that the chemical reactions inside the cylinder might have occurred earlier than that in C1. These early chemical reactions might be due to the higher internal EGR temperature resulted from the greater BMEP in C2. In addition, the AFR in C2 was 15.5:1, while the AFR in C1 was 16:1. The increased richness of the mixture in C2 might also have partly contributed to the early occurrence of the chemical reactions.

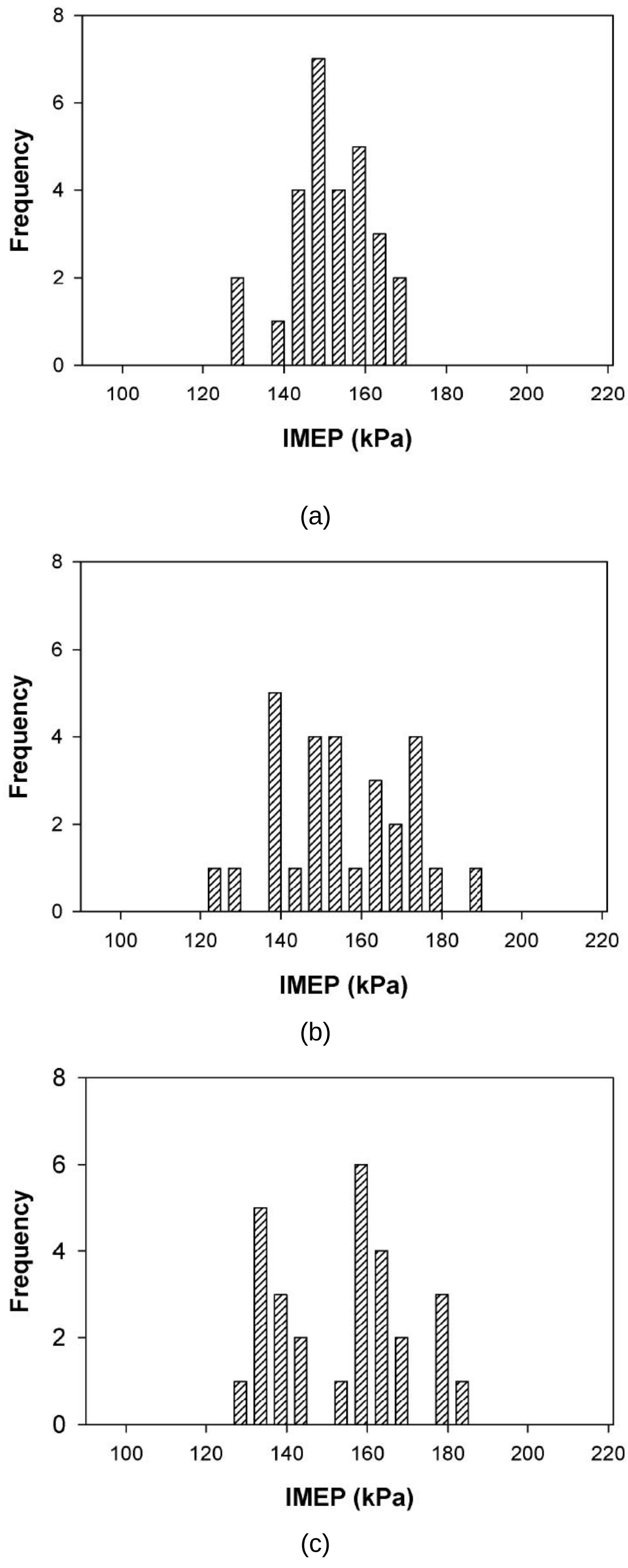

Figure 8: Histograms if IMEP in test condition C2, (a) SA-AI-45, spark timing 45^0 BTDC and (b) SA-AI-22, spark timing 22^0 BTDC and (c) AI without spark assistance

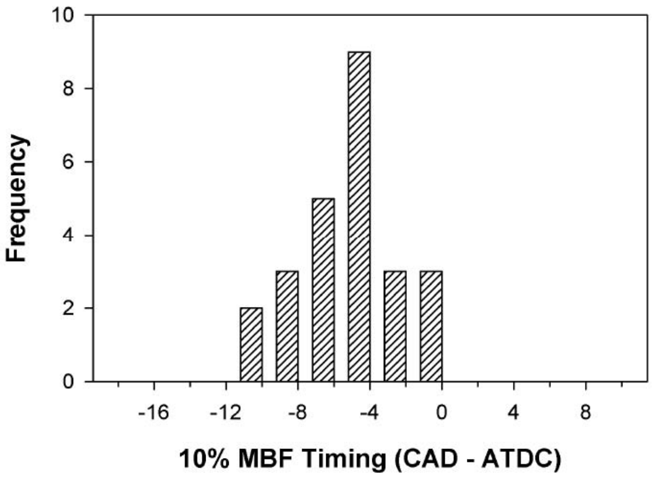

(a)

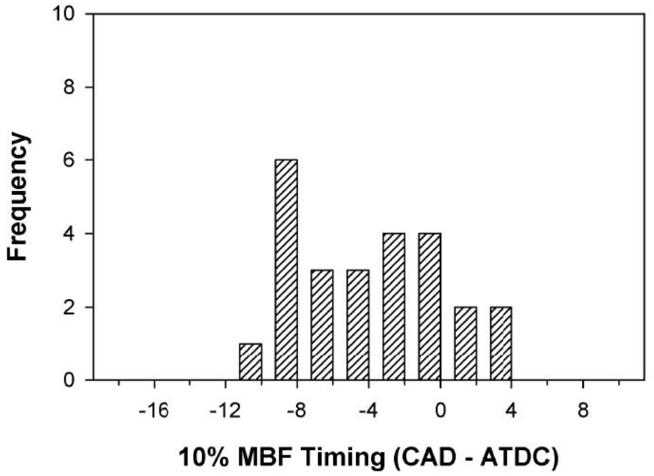

(b)

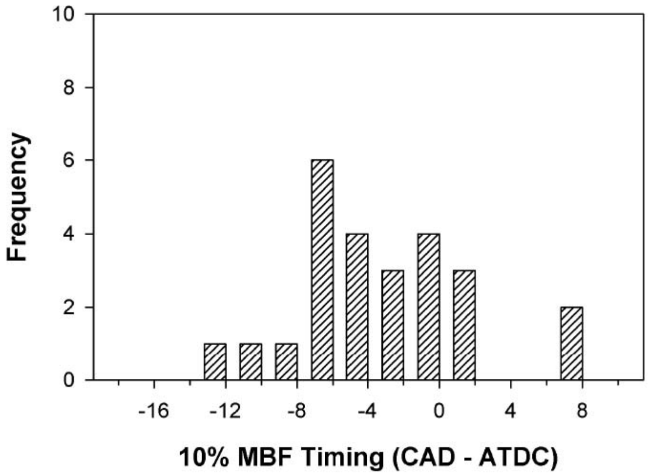

(c)

Figure 9: Histograms of 10% MBF timing in test condition C2 (a) SA-AI-45, spark timing 450 BTDC (b) SA-AI-22, spark timing 220 BTDC and (c) AI without spark assistance

Table 3 summarizes the results of the SA-AI-45, and AI mode operations under condition C2. The results in test condition C2 show the influence of spark timing to the spark assistance's effect on improving the cyclic variation in AI mode at light load conditions. However, at a fixed engine operating condition, the spark assistance is only effective when the spark timing is sufficiently advanced. The advancement of the spark timing required to make the spark assistance effective may vary with engine load and AFR.

Table 3: Condition C2 summary

	SA-AI-45	SA-AI-22	AI
CoV of IMEP	6.6%	10.4%	10.8%
Standard deviation of 10% MBF timing	2.7^0	3.4^0	4.7^0

CONCLUSION

The effect of spark assistance on the cyclic stability of the AI at light engine load operation was investigated experimentally on a two-stroke single cylinder engine. Two experimental conditions were designated, one at a load condition (BMEP-140kPa) which was at the edge of the AI lower limit (C1) and the other at BMEP of 150kPa which was slightly above the AI lower limit (C2). C1 was aimed to investigate the effect of spark assistance on the cyclic variation at light engine loads, while C2 was aimed to investigate the effect of the spark timing on spark assisted AI. The outcomes of this work can be concluded as follows:

1. When SA-AI was applied to the engine operating condition C1, the cyclic variations of the peak cylinder pressure and 10% MBF timing were significantly reduced.

2. In engine test condition C1, the effect of the spark assistance on IMEP was not as significant as that on the peak cylinder pressure and 10% MBF.

3. In engine test condition C2, 10% MBF timing occurred at a relatively advanced crank angle. Thus the effect of SA-AI timing on the 10% MBF timing and IMEP at 22^0 before TDC was less than that at 45^0 before TDC. The reason was presumed to be the early occurrence of chemical reactions leading to AI.

ACKNOWLEDGMENTS

The authors are grateful to Mr. Harold Myers, Mr. Bill Firth and Mr. Scott Graham for their continuous support for the fabrication of components required for setting up the experiments.

REFERENCES

1. Y. Ishibashi. Basic Understanding of Activated Radical Combustion and its Two-Stroke Engine Application and Benefits SAE paper 2000-01-1836, 2000
2. S. Onishi, S. Hong Jo, K. Shoda, Pan Do Jo, and S. Kato. "Active thermo-atmosphere combustion (ATAC) - A new combustion process for internal combustion engines". SAE paper 790501, 1979
3. Z. Wang, J. Wang, S. Shuai, G. Tian, X. An, and Q. Ma. Study of the effect of spark ignition on gasoline HCCI combustion. Proceedings of IMechE, Part D:

Journal of Automobile Engineering, 220:817–825, 2006.
4. Z. Wang, J. Wang, S. Shuai, and Q. Ma. New gasoline homogeneous charge compression ignition combustion system using two-state direct injection and assisted spark ignition. Proceedings of IMechE, Part D: Journal of Automobile Engineering, 220:367–377, 2006.
5. J. Yang. Expanding the operating range of homogeneous charge compression ignition spark ignition dual-mode engines in the homogeneous charge compression ignition mode. International Journal of Engine Research, IMechE, 6:279–288, 2005.
6. William J. Glewen, Robert M. Wagner, K. Dean Edwards, and C. Stuart Daw. Analysis of cyclic variability in spark-assisted HCCI combustion using a double Wiebe function. Proceedings of the Combustion Institute, In Press, Corrected Proof:–, 2009.
7. Janitha S. Wijesinghe, Guang Hong, "Experimental investigation of spark assisted auto-ignition combustion in a small two-stroke engine", SAE paper 2008-01-1665.

CONTACT

Janitha Wijesinghe
Research Student in Mechanical Engineering
Faculty of Engineering
University of Technology Sydney
PO Box 123, Broadway, NSW 2007,
Australia

Email: Janitha.Wijesinghe@eng.uts.edu.au

NOMENCLATURE

AI – Auto Ignition

SI – Spark Ignition

HCCI – Homogeneous Charge Compression Ignition

SA-AI – Spark Assisted Auto Ignition

EGR – Exhaust Gas Recirculation

IMEP – Indicated Mean Effective Pressure

BMEP – Brake Mean Effective Pressure

AFR – Air to Fuel Ratio

RPM – Revolutions Per Minute

TDC – Top Dead Centre

BTDC – Before Top Dead Centre

ATDC – After Top Dead Centre

CoV – Coefficient of Variation